Natural Convection-Radiation Interaction in Boundary-Layer Flow over Horizontal Surfaces

M.M. Ali,* T.S. Chen,† and B.F. Armaly†
University of Missouri-Rolla, Rolla, Missouri

The interaction of natural convection with thermal radiation in laminar boundary-layer flow over an isothermal, horizontal flat plate is studied analytically. The fluid considered is a gray, absorbing-emitting but nonscattering medium, and the Rosseland approximation is used to describe the radiative heat flux in the energy equation. Both a hot surface facing upward and a cold surface facing downward are considered in the analysis. The conservation equations that govern the problem are reduced to a system of nonlinear ordinary differential equations. The resulting boundary-value problem is then solved by a Runge-Kutta integration scheme in conjunction with the Newton-Raphson shooting method. The important parameters of this problem are the Grashof and Prandtl numbers, the radiation-conduction parameter M, and the freestream-to-wall temperature ratio T_∞/T_w for the case of a hot surface or the wall-to-freestream temperature ratio T_w/T_∞ for the case of a cold surface. Numerical results are presented for gases with a Prandtl number of 0.7 for both hot and cold surfaces, with values of M ranging from 0 to 50 and the T_∞/T_w or T_w/T_∞ ratio from 0 to 1.0. In general, it is found that both the wall shear stress and the surface heat-transfer rate increase with increasing radiation interaction (i.e., increasing value of M) for both a hot surface facing upward with $T_w > T_\infty$ and a cold surface facing downward with $T_w < T_\infty$.

Nomenclature

F = reduced streamfunction, $= \psi(x, y)/[5\nu(Gr_x/5)^{1/5}]$
g = gravitational acceleration
Gr_x = local Grashof number, $= g\beta|T_w - T_\infty|x^3/\nu^2$
k = thermal conductivity
M = radiation-conduction parameter, $= 4\sigma T_w^3/k\kappa$ or $4\sigma T_\infty^3/k\kappa$
Nu_x = local Nusselt number, $= q_w x/[k(T_w - T_\infty)]$
Pr = Prandtl number, $= \nu/\alpha$
q_r = local radiative heat flux
q_w = local surface heat flux
T = temperature
T_0 = reference temperature
u, v = axial and normal velocity components
x, y = axial and normal coordinates
α = thermal diffusivity
β = volumetric coefficient of thermal expansion
η = similarity variable, $= (y/x)(Gr_x/5)^{1/5}$
θ = dimensionless temperatures, $= T/T_w$ or T/T_∞
κ = mean absorption coefficient
μ = dynamic viscosity
ν = kinematic viscosity
σ = Stefan-Boltzmann constant
τ_w = local wall shear stress
ϕ = dimensionless temperature, $= (T - T_\infty)/(T_w - T_\infty)$
ψ = streamfunction

Subscripts

w = condition at wall
∞ = condition at freestream

Introduction

HEAT transfer by natural convection in laminar boundary-layer flows has been analyzed extensively for semi-infinite flat plate in vertical, horizontal, and inclined orientations. Typical studies can be found, for example, in Refs. 1-4. On the other hand, heat transfer by simultaneous natural convection and thermal radiation in a participating fluid has not received as much attention. This is unfortunate, because thermal radiation will play a significant role in the overall surface heat transfer in situations where convective heat-transfer coefficients are small, as is the case in natural convection. The majority of studies dealing with the interaction of thermal radiation and natural convection have been confined to the case of a vertical semi-infinite plate (see, e.g., Refs. 5-9).

To the authors' knowledge, no study exists on radiation interaction with natural convection in boundary-layer flow over a horizontal or inclined surface. This has motivated the present study. In this paper, such a boundary-layer flow over a semi-infinite horizontal plate is presented. The boundary layer is formed in this flow configuration when the hot surface is facing upward or when the cold surface is facing downward. In the analysis, consideration is given to gray gases that emit and absorb but do not scatter thermal radiation. The mathematical problem that arises in a general analysis of such a problem is quite complex. For this reason, a further simplification is introduced in the present analysis by utilizing the Rosseland approximation to describe the radiative heat flux in the medium. This approximation is valid at points optically far from the bounding surface, and is good only for intensive absorption, that is, for an optically thick boundary layer. In spite of these shortcomings, the Rosseland approximation has been used with success in a variety of problems ranging from transport of radiation through gases at low density to the study of the effects of radiation on blast waves by nuclear explosions. The objective of this study is to provide the first results on natural convection-radiation interaction in boundary-layer flow over a horizontal semi-infinite flat plate, which can be used for comparisons with future studies that will consider a more accurate expression for the radiative heat flux.

The conservation equations are first transformed into a system of nonlinear ordinary differential equations which are then solved simultaneously by Runge-Kutta integration scheme in conjunction with Newton-Raphson shooting technique to determine the unknown quantities. The important parameters in the problem are the local Grashof number, the Prandtl number, the radiation-conduction parameter, and the freestream-to-wall or the wall-to-freestream temperature ratio.

Presented as Paper 82-0917 at the AIAA/ASME Third Joint Thermophysics Fluids, Plasma and Heat Transfer Conference, St. Louis, Mo., June 7-11, 1982; received Aug. 17, 1983; revision received Feb. 22, 1984.

*Graduate Student.
†Professor of Mechanical Engineering, Department of Mechanical and Aerospace Engineering. Member AIAA.

Numerical results for the local wall shear stress, the local surface heat flux, and the local Nusselt number, as well as the velocity and temperature distribution, are presented for gases with a Prandtl number of 0.7 for various values of the radiation-conduction parameter and the freestream-to-wall or the wall-to-freestream temperature ratio. They cover results for hot surfaces facing upward and cold surfaces facing downward.

Analysis

Consider a semi-infinite flat plate that is maintained at a uniform temperature T_w and is placed horizontally in a quiescent fluid of infinite extent at a constant temperature T_∞. The fluid is assumed to be a gray, emitting and absorbing, but nonscattering medium. The physical coordinates (x, y) are chosen such that x is measured from the leading edge of the plate in the streamwise direction and y is measured normal to the surface of the plate. The radiative heat flux in the x direction is considered negligible in comparison with that in the y direction.[10] In addition, the viscous dissipation and the axial heat conduction effects are neglected. The properties of the fluid are assumed to be constant, except for the density variation in the y direction that induces the buoyancy force. Under these assumptions, along with the Boussinesq approximation, the conservation equations for the steady, two-dimensional laminar boundary-layer flow problem under consideration can be written as

$$\frac{\partial u}{\partial x}+\frac{\partial v}{\partial y}=0 \tag{1}$$

$$u\frac{\partial u}{\partial x}+v\frac{\partial u}{\partial y}=\nu\frac{\partial^2 u}{\partial y^2}\pm g\beta\frac{\partial}{\partial x}\int_y^\infty (T-T_\infty)\mathrm{d}y \tag{2}$$

$$u\frac{\partial T}{\partial x}+v\frac{\partial T}{\partial y}=\alpha\left(\frac{\partial^2 T}{\partial y^2}-\frac{1}{k}\frac{\partial q_r}{\partial y}\right) \tag{3}$$

In the above equations, the conventional notations are defined in the Nomenclature. The second term on the right-hand side of Eq. (2) is the streamwise pressure gradient induced by the buoyancy force, with the plus sign pertaining to fluid above the plate and the minus sign to fluid below the plate. It should be noted that for the problem under consideration, the boundary layer will form only either when the hot surface is facing upward with $T_w > T_\infty$ or when the cold surface is facing downward with $T_w < T_\infty$. The quantity q_r on the right-hand side of Eq. (3) represents the radiative heat flux in the y direction. In order to reduce the complexity of the problem and to provide a means of comparison with future studies that will employ a more detailed representation for the radiative heat flux, the optically thick radiation limit is considered in the present analysis. Thus, the radiative heat flux term is simplified by using the Rosseland approximation[10] as

$$q_r=-\frac{4\sigma}{3\kappa}\frac{\partial T^4}{\partial y} \tag{4}$$

which is valid only for intensive absorption. The boundary conditions for Eqs. (1-3) are

$$\begin{aligned} &u=v=0, \quad T=T_w \quad \text{at } y=0\\ &u\to 0, \quad T\to T_\infty \quad \text{as } y\to\infty \end{aligned} \tag{5}$$

Equations (1-3) and (5), along with Eq. (4), can be reduced to a system of ordinary differential equations by introducing a similarity variable η, a reduced streamfunction $F(\eta)$, and a dimensionless temperature $\theta(\eta)$ defined, respectively, as

$$\eta=(y/x)(Gr_x/5)^{1/5}, \quad \psi(x,y)=5\nu(Gr_x/5)^{1/5}F(\eta) \tag{6}$$

$$\theta(\eta)=T/T_w \text{ for hot surfaces} \tag{7a}$$

$$=T/T_\infty \text{ for cold surfaces} \tag{7b}$$

where the local Grashof number Gr_x is defined as

$$Gr_x=g\beta|T_w-T_\infty|x^3/\nu^2 \tag{8}$$

and the streamfunction $\psi(x, y)$ satisfies the continuity Eq. (1) with

$$u=\frac{\partial\psi}{\partial y}, \qquad v=-\frac{\partial\psi}{\partial x} \tag{9}$$

Introduction of Eqs. (6), (7), and (9) into Eqs. (1-4) results in

$$\frac{\mathrm{d}^3F}{\mathrm{d}\eta^3}+3F\frac{\mathrm{d}^2F}{\mathrm{d}\eta^2}-\left(\frac{\mathrm{d}F}{\mathrm{d}\eta}\right)^2+\frac{2}{5}\left(\eta\phi+\int_\eta^\infty\phi\,\mathrm{d}\eta\right)=0 \tag{10}$$

$$\frac{1}{Pr}\frac{\mathrm{d}}{\mathrm{d}\eta}\left[\left(1+\frac{4}{3}M\theta^3\right)\frac{\mathrm{d}\theta}{\mathrm{d}\eta}\right]+3F\frac{\mathrm{d}\theta}{\mathrm{d}\eta}=0 \tag{11}$$

where Pr is the Prandtl number, M is the radiation-conduction parameter expressed as

$$M=\frac{4\sigma T_w^3}{k\kappa} \quad \text{for hot surfaces} \tag{12a}$$

$$=\frac{4\sigma T_\infty^3}{k\kappa} \quad \text{for cold surfaces} \tag{12b}$$

and

$$\phi=\frac{\theta-(T_\infty/T_w)}{1-(T_\infty/T_w)} \quad \text{for hot surfaces} \tag{13a}$$

$$=\frac{\theta-1}{(T_w/T_\infty)-1} \quad \text{for cold surfaces} \tag{13b}$$

in which $\theta=T/T_w$ for hot surfaces and $\theta=T/T_\infty$ for cold surfaces as defined in Eq. (7). Thus, the ϕ expressions for both hot and cold surfaces reduce to $(T-T_\infty)/(T_w-T_\infty)$. The boundary conditions, Eq. (5), are transformed as follows for the case of hot surface

$$\begin{aligned} &F=\frac{\mathrm{d}F}{\mathrm{d}\eta}=0 \quad \text{and} \quad \theta=1 \quad \text{at } \eta=0\\ &\frac{\mathrm{d}F}{\mathrm{d}\eta}\to 0 \quad \text{and} \quad \theta\to\frac{T_\infty}{T_w} \quad \text{as } \eta\to\infty \end{aligned} \tag{14a}$$

and for the case of cold surfaces

$$\begin{aligned} &F=\frac{\mathrm{d}F}{\mathrm{d}\eta}=0 \quad \text{and} \quad \theta=\frac{T_w}{T_\infty} \quad \text{at } \eta=0\\ &\frac{\mathrm{d}F}{\mathrm{d}\eta}\to 0 \quad \text{and} \quad \theta\to 1 \quad \text{as } \eta\to\infty \end{aligned} \tag{14b}$$

It should be noted that M as defined in Eq. (12) is the inverse of the conduction-radiation parameter N commonly used in the literature. When $M=0$ there is no radiation interaction, and Eqs. (10), (11), and (14) reduce to those for pure natural convection flow over a horizontal flat plate.[2] The radiation interaction with convection increases with increasing values of M. It is further noted that with the use of the absolute value $|T_w-T_\infty|$ in the definition of Gr_x in Eq. (8), the plus sign preceding 2/5 in the last group of terms in Eq. (10) applies to both $T_w > T_\infty$ for a hot surface facing upward and $T_w < T_\infty$ for a cold surface facing downward. Equations (10) and (11) are two coupled nonlinear ordinary differential equations for the functions $F(\eta)$ and $\theta(\eta)$, with Pr, M, and T_∞/T_w or T_w/T_∞ as the parameters. Thus, they must be

solved simultaneously, subject to the boundary conditions, Eq. (14a) or (14b).

In situations where the wall temperature T_w is not very much different from the freestream temperature T_∞, the T^4 term appearing in the q_r expression in Eq. (4) may be expressed as a linear function of temperature by expanding T^4 in a Taylor series about a reference temperature T_0 and neglecting higher order terms. Thus,

$$T^4 \approx 4T_0^3 T - 3T_0^4 \tag{15}$$

With this, the transformed energy equation assumes the form

$$\frac{1}{Pr}\left(1+\frac{4}{3}M\right)\frac{d^2\theta}{d\eta^2} + 3F\frac{d\theta}{d\eta} = 0 \tag{16}$$

for both hot and cold surfaces, with M and θ both based on T_0. For a hot surface T_0 is taken as T_w, whereas for a cold surface T_0 is taken as T_∞.

The physical quantities of interest are the local wall shear stress τ_w, the local surface heat flux q_w, the velocity distribution $dF/d\eta$ and the temperature distribution $\theta(\eta)$. From the definitions of τ_w and q_w

$$\tau_w = \mu\left(\frac{\partial u}{\partial y}\right)_{y=0}, \qquad q_w = -k\left(\frac{\partial T}{\partial y}\right)_{y=0} - \frac{4\sigma}{3\kappa}\left(\frac{\partial T^4}{\partial y}\right)_{y=0} \tag{17}$$

together with the definition of the local Nusselt number Nu_x

$$Nu_x = \frac{q_w}{T_w - T_\infty}\frac{x}{k} \tag{18}$$

one can write

$$\tau_w \frac{x^2}{5\mu\nu}\left(\frac{Gr_x}{5}\right)^{-3/5} = \left(\frac{d^2F}{d\eta^2}\right)_{\eta=0} \tag{19}$$

$$q_w = -\frac{k}{x}T_0\left\{1+\frac{4}{3}M[\theta(0)]^3\right\}\left(\frac{Gr_x}{5}\right)^{1/5}\left(\frac{d\theta}{d\eta}\right)_{\eta=0} \tag{20}$$

$$Nu_x\left(\frac{Gr_x}{5}\right)^{-1/5} = \frac{1+(4/3)M[\theta(0)]^3}{A}\left[-\left(\frac{d\theta}{d\eta}\right)\right]_{\eta=0} \tag{21}$$

where θ and M are defined, respectively, by Eqs. (7) and (12), and $A = 1 - T_\infty/T_w$ for a hot surface and $A = T_w/T_\infty - 1$ for a cold surface. For the case of T^4 linearized, the corresponding q_w and Nu_x expressions can be easily obtained. They assume, respectively, the form of Eqs. (20) and (21) except that for this case $\theta(0)$ is replaced by 1.

The velocity distribution u is related to $dF/d\eta$ through the expression

$$\frac{ux}{\nu} = 5\left(\frac{Gr_x}{5}\right)^{2/5}\frac{dF}{d\eta} \tag{22}$$

and the temperature distribution is given by Eq. (7a) for hot surfaces and by Eq. (7b) for cold surfaces.

Numerical Method of Solution

The system of Eqs. (10), (11), and (14) was solved numerically by the Runge-Kutta integration scheme for values of the radiation-conduction parameter M ranging from 0 to 50 and the temperature ratio T_∞/T_w or T_w/T_∞ between 0 and 1.0 for gases having a Prandtl number of 0.7. In the numerical solution, the integral appearing in Eq. (10) was removed by introducing a new function $G(\eta)$ as

$$G = \int_\eta^\infty \phi\, d\eta \tag{23}$$

with ϕ as a function of θ given by Eq. (13), such that an additional equation

$$\frac{dG}{d\eta} + \phi = 0, \qquad G \to 0 \quad \text{as } \eta \to \infty \tag{24}$$

results. Thus, the numerical integration was performed on Eqs. (10), (11), and (24) to solve simultaneously for the F, θ, and G functions and to determine the unknown quantities $d^2F/d\eta^2$, $d\theta/d\eta$, and G at $\eta = 0$ (i.e., at the surface of the plate). These unknown quantities were obtained by employing a modified version of the Newton-Raphson shooting method. In the numerical integration, a step size of $\Delta\eta = 0.02$ was used and the value of η_∞ (an approximation to $\eta = \infty$) was varied systematically until the conditions at $\eta = \eta_\infty$ were satisfied within a specified tolerance of less than 5×10^{-4}. The solution was obtained by starting with $M = 0$ (no radiation interaction); then M was increased gradually to 50 for each value of T_∞/T_w or T_w/T_∞.

Results and Discussion

The numerical results for $d^2F/d\eta^2$ and $d\theta/d\eta$ at $\eta = 0$, denoted by $F''(0)$ and $\theta'(0)$, respectively, were obtained for representative values of $M = 4\sigma T_w^3/k\kappa$ between 0 and 50 and $0 \le T_\infty/T_w < 1.0$ for the case of the hot surface and for $M = 4\sigma T_\infty^3/k\kappa$ between 0 and 50 and $0 \le T_w/T_\infty < 1.0$ for the case of the cold surface. The Prandtl number was taken to be 0.7 for both cases. It is noted here that for both carbon dioxide in the temperature range 100 ~ 650°F (with corresponding Prandtl number range 0.76 ~ 0.6) and ammonia vapor in the temperature range 120 ~ 400°F (with Pr in the range 0.88 ~ 0.84) at 1 atm, the values of M range approximately from 10 to 30, whereas for water vapor in the temperature range 220 ~ 900°F (with $Pr \sim 1.0$) the M values lie between 30 and 200 (see Ref. 12).

It must be emphasized that the value of $F''(0)$ is not a direct measure of the local wall shear stress τ_w, nor is the value of $\theta'(0)$ a direct measure of the local surface heat flux q_w. The local wall shear stress is related to $F''(0)$ through Eq. (19), the local surface heat flux is related to $\theta'(0)$ through Eq. (20), and the local Nusselt number Nu_x is related to $\theta'(0)$ through Eq. (21). However, these equations contain the Grashof number Gr_x that is based on the temperature difference $|T_w - T_\infty|$, which in turn varies with varying temperature ratio T_∞/T_w or T_w/T_∞. Thus, to properly present the effects of the radiation-conduction parameter M and the T_∞/T_w or T_w/T_∞ ratio on the local wall shear stress and the local surface heat transfer, the Grashof number in the τ_w, q_w, and Nu_x expressions is redefined based on a reference temperature T_0 as

$$Gr_x^* = g\beta T_0 x^3/\nu^2 \tag{25}$$

In terms of the modified Grashof number Gr_x^*, the expressions for τ_w, q_w, and Nu_x become, respectively,

$$\tau_w \frac{x^2}{5\mu\nu}\left(\frac{Gr_x^*}{5}\right)^{-3/5} = \left|\frac{T_w - T_\infty}{T_0}\right|^{3/5} F''(0) \tag{26}$$

$$q_w = -\frac{k}{x}T_0\left\{1+\frac{4}{3}M[\theta(0)]^3\right\}\left(\frac{Gr_x^*}{5}\right)^{1/5}\left|\frac{T_w - T_\infty}{T_0}\right|^{1/5}\theta'(0) \tag{27}$$

and

$$\frac{q_w x}{T_0 k}\left(\frac{Gr_x^*}{5}\right)^{-1/5} = \left\{1+\frac{4}{3}M[\theta(0)]^3\right\} \times \left|\frac{T_w - T_\infty}{T_0}\right|^{1/5}[-\theta'(0)] \tag{28}$$

Table 1 $F''(0)$ and $\theta'(0)$ results for the case of hot surface, $Pr = 0.7$ ($\theta = T/T_w$)

	$T_\infty/T_w = 0$		0.2		0.4		0.5		0.6		0.8	
$M = 4\sigma T_w^3/k\kappa$	$F''(0)$	$-\theta'(0)$	$F''(0)$	$-\theta'(0)$	$F''(0)$	$-\theta'(0)$	$F''(0)$	$-\theta'(0)$	$F''(0)$	$-\theta'(0)$	$F''(0)$	$-\theta'(0)$
0	0.5192	0.4891	0.5192	0.3913	0.5192	0.2935	0.5192	0.2446	0.5192	0.1956	0.5192	0.0978
0.05	0.5236	0.4665	0.5244	0.3744	0.5255	0.2819	0.5262	0.2356	0.5270	0.1890	0.5291	0.0952
0.10	0.5279	0.4465	0.5295	0.3593	0.5317	0.2717	0.5331	0.2276	0.5347	0.1831	0.5388	0.0928
0.50	0.5601	0.3426	0.5673	0.2810	0.5772	0.2178	0.5834	0.1851	0.5905	0.1514	0.6076	0.0797
1.0	0.5956	0.2774	0.6085	0.2312	0.6262	0.1828	0.6371	0.1571	0.6494	0.1301	0.6781	0.0702
2.5	0.6829	0.1966	0.7085	0.1681	0.7428	0.1370	0.7636	0.1197	0.7860	0.1008	0.8349	0.0562
5	0.7941	0.1489	0.8344	0.1296	0.8870	0.1078	0.9173	0.0952	0.9507	0.0810	1.0211	0.0460
10	0.9593	0.1127	1.0183	0.0996	1.0920	0.0841	1.1341	0.0749	1.1775	0.0641	1.2696	0.0368
15	1.0864	0.0959	1.1575	0.0853	1.2448	0.0726	1.2931	0.0648	1.3434	0.0556	1.4467	0.0321
20	1.1918	0.0856	1.2715	0.0764	1.3680	0.0653	1.4218	0.0584	1.4770	0.0502	1.5922	0.0290
25	1.2826	0.0784	1.3692	0.0701	1.4732	0.0601	1.5301	0.0538	1.5900	0.0463	1.7130	0.0268
30	1.3627	0.0729	1.4551	0.0654	1.5655	0.0561	1.6264	0.0503	1.6892	0.0433	1.8194	0.0251
40	1.5006	0.0652	1.6021	0.0586	1.7234	0.0504	1.7892	0.0452	1.8574	0.0390	1.9973	0.0226
50	1.6174	0.0597	1.7264	0.0538	1.8569	0.0464	1.9268	0.0416	1.9992	0.0359	2.1464	0.0208

Table 2 $F''(0)$ and $\theta'(0)$ results for the case of cold surface, $Pr = 0.7$ ($\theta = T/T_\infty$)

	$T_w/T_\infty = 0$		0.2		0.4		0.5		0.6		0.8	
$M = 4\sigma T_\infty^3/k\kappa$	$F''(0)$	$\theta'(0)$	$F''(0)$	$\theta'(0)$	$F''(0)$	$\theta'(0)$	$F''(0)$	$\theta'(0)$	$F''(0)$	$\theta'(0)$	$F''(0)$	$\theta'(0)$
0	0.5192	0.4891	0.5192	0.3913	0.5192	0.2935	0.5192	0.2446	0.5192	0.1956	0.5192	0.0978
0.05	0.5214	0.4925	0.5221	0.3949	0.5233	0.2964	0.5241	0.2468	0.5252	0.1971	0.5283	0.0977
0.10	0.5236	0.4960	0.5250	0.3984	0.5274	0.2993	0.5291	0.2490	0.5312	0.1984	0.5369	0.0975
0.50	0.5406	0.5224	0.5474	0.4259	0.5577	0.3202	0.5654	0.2639	0.5746	0.2064	0.5980	0.0953
1.0	0.5595	0.5532	0.5722	0.4577	0.5919	0.3425	0.6058	0.2780	0.6223	0.2124	0.6609	0.0920
2.5	0.6068	0.6370	0.6344	0.5420	0.6761	0.3910	0.7038	0.3021	0.7354	0.2171	0.8077	0.0832
5	0.6704	0.7616	0.7155	0.6593	0.7838	0.4373	0.8250	0.3144	0.8725	0.2109	0.9779	0.0730
10	0.7675	0.9779	0.8375	0.8426	0.9389	0.4727	0.9976	0.3094	1.0649	0.1930	1.2054	0.0612
15	0.8439	1.1691	0.9332	0.9839	1.0550	0.4792	1.1260	0.2964	1.2052	0.1781	1.3720	0.0544
20	0.9084	1.3441	1.0099	1.0950	1.1483	0.4753	1.2308	0.2834	1.3174	0.1662	1.5024	0.0496
25	0.9640	1.5059	1.0781	1.1868	1.2307	0.4680	1.3187	0.2713	1.4157	0.1569	1.6140	0.0461
30	1.0151	1.6599	1.1374	1.2621	1.3017	0.4588	1.3985	0.2610	1.5005	0.1491	1.7169	0.0435
40	1.1022	1.9432	1.2403	1.3786	1.4248	0.4398	1.5327	0.2432	1.6455	0.1369	1.8781	0.0393
50	1.1770	2.2045	1.3282	1.4629	1.5294	0.4221	1.6431	0.2288	1.7650	0.1276	2.0218	0.0364

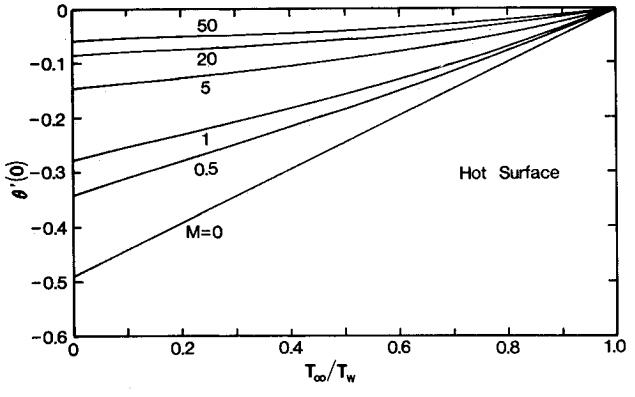

Fig. 1 Temperature gradient at the wall for a hot surface ($\theta = T/T_w$).

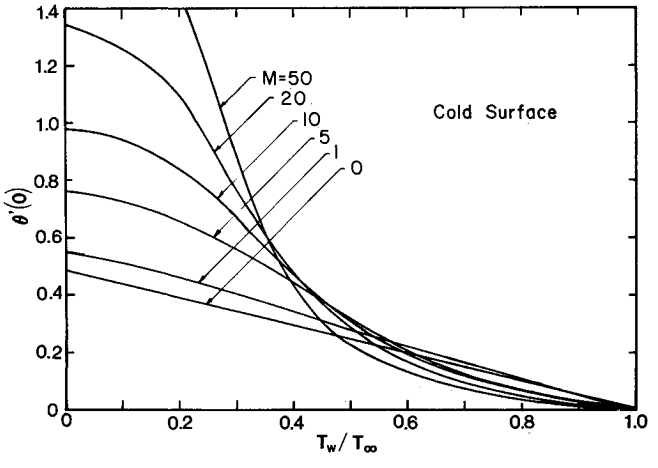

Fig. 2 Temperature gradient at the wall for a cold surface ($\theta = T/T_\infty$).

The quantity $q_w x/T_0 k$ in Eq. (28) is the modified local Nusselt number Nu_x^*. The reference temperature T_0 in the preceding equations is taken as T_w for the case of the hot surface and as T_∞ for the case of the cold surface. It should also be noted that $\theta(0)$ becomes 1 and T_w/T_∞, respectively, for the hot and cold surfaces, because $\theta = T/T_w$ for the former and $\theta = T/T_\infty$ for the latter.

The $F''(0)$ and $\theta'(0)$ results are listed in Table 1 for the case of the hot surface and in Table 2 for the case of the cold surface. The $F''(0)$ and $\theta'(0)$ values for the case of $M = 0$ (i.e., pure natural convection without the interaction of thermal radiation) agree exactly with the results of Chen and Tzuoo.[4] To better illustrate the behavior of the wall temperature gradient $\theta'(0)$ as a function of T_∞/T_w for the hot surface and of T_w/T_∞ for the cold surface, with M as a parameter, Figs. 1 and 2 have been prepared. For small values of M the heat transfer is dominated by conduction, and the curves are seen to be practically linear with T_∞/T_w or T_w/T_∞. As the thermal radiation becomes the dominant mode of heat transfer (i.e., when the values of M are large), the curves depart more from the linearity as M increases. The general trend of the curves is that, for a given value of M, the wall temperature gradient (i.e., the conductive heat flux at the wall) has a maximum absolute value when the temperature ratio T_∞/T_w or T_w/T_∞ is equal to zero [i.e., when $(T_w - T_\infty)$ is maximum] and decreases to zero when the temperature ratio becomes unity [i.e., when

$(T_w - T_\infty) = 0$]. It should also be pointed out that, similar to what was observed by Viskanta and Grosh,[11] for the case of a cold surface, Fig. 2, the effect of radiation is to decrease the conductive wall heat flux $\theta'(0)$ below the nonradiating medium case ($M = 0$) when T_w/T_∞ is approximately larger than 0.5 and to increase it above the nonradiating medium case when T_w/T_∞ is less than 0.5. For hot surfaces, Fig. 1, the conductive heat flux at the wall is always lower than the case of nonradiating medium for all values of T_∞/T_w. The total surface heat transfer rate (conductive plus radiative), however, is always increasing with increasing radiation-conduction parameters for both hot and cold surfaces, as can be seen from Figs. 3 and 4.

The local surface heat flux or the local Nusselt number in the form of $(q_w x/kT_w)(Gr_x^*/5)^{-1/5}$ is presented as a function of T_∞/T_w, with $M = 4\sigma T_w^3/k\kappa$ as a parameter, for the case of the hot surface facing upward in Fig. 3. It can be seen from the figure that for values of M close to 0 the curves are almost a linear function of T_∞/T_w, which is a characteristic feature of a conduction dominated regime. As the value of M increases, the interaction of thermal radiation intensifies and the surface heat flux increases. As is to be expected, for a given value of M, the surface heat flux is maximum when $T_\infty/T_w = 0$ [i.e., when $(T_w - T_\infty)$ is maximum] and decreases to 0 when $T_\infty/T_w = 1$ (i.e., when $T_w - T_\infty = 0$). The local surface heat flux for the case of the cold surface facing downward in the form of $(q_w x/kT_\infty)(Gr_x^*/5)^{-1/5}$ is presented as a function of T_w/T_∞ in Fig. 4, with $M = 4\sigma T_\infty^3/k\kappa$ as a parameter. The behavior and the trend of the curves are similar to those for the case of the hot surface except that the surface heat flux has a negative value. This is due to the fact that heat is transferred from the ambient fluid to the cold wall in a direction opposite to the positive y coordinate. Again, it is seen that the interaction of thermal radiation enhances the local surface heat flux and that for a given value of M the surface heat flux decreases from a maximum value at $T_w/T_\infty = 0$ to a minimum value of 0 at $T_w/T_\infty = 1$.

A comparison of the surface heat flux results between the hot and cold surfaces, Figs. 3 and 4, reveals that for the same value of M, a hot surface that is facing upward provides a larger surface heat flux than a cold surface that is facing downward. For example, for a hot surface with $T_\infty/T_w = 0.5$ and $M = 20$, the value of $(q_w x/kT_w)(Gr_x^*/5)^{-1/5}$ is 1.407, whereas for a cold surface with $T_w/T_\infty = 0.5$ and $M = 20$, the value of $(q_w x/kT_\infty)(Gr_x^*/5)^{-1/5}$ is -1.069. The reason for this behavior can be explained by examining the radiative flux term in the surface heat flux expression, Eq. (28). At the wall, the radiative flux term $(4/3)M[\theta(0)]^3[-\theta'(0)]$ becomes $(4/3)M[-\theta'(0)]$ for the hot surface and $(4/3)M(T_w/T_\infty)^3[-\theta'(0)]$ for the cold surface. Since $T_w/T_\infty < 1$, the interaction of thermal radiation will then be felt stronger with a hot surface than with a cold surface, thus resulting in a higher surface heat flux.

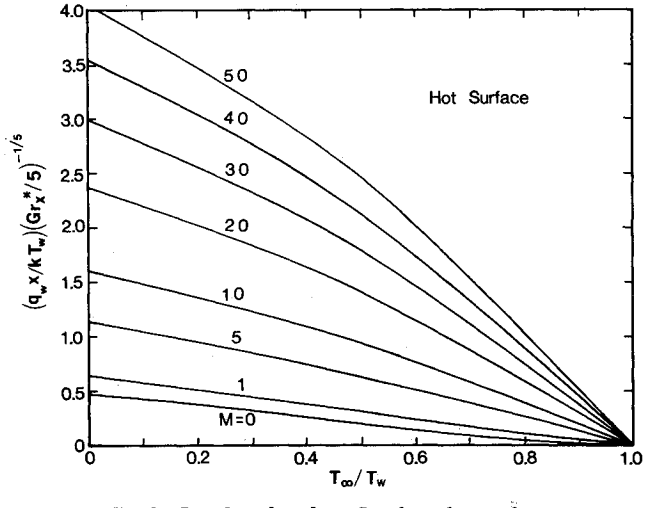

Fig. 3 Local surface heat flux for a hot surface.

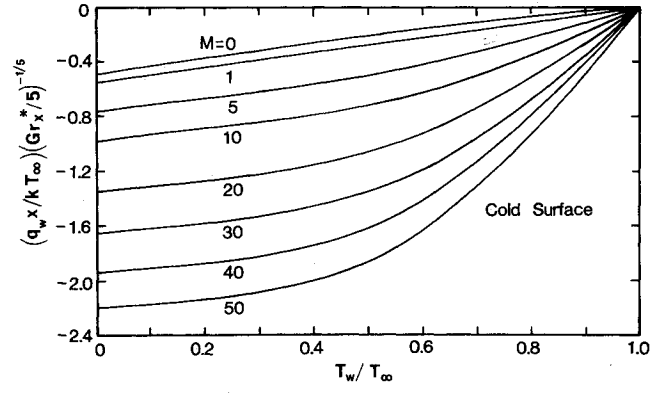

Fig. 4 Local surface heat flux for a cold surface.

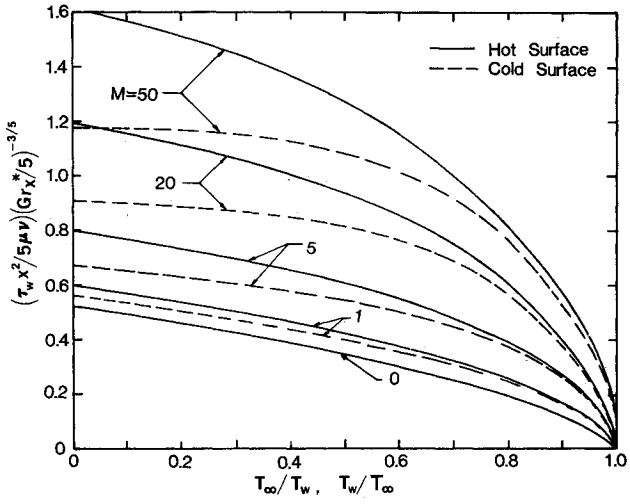

Fig. 5 Local wall shear stress.

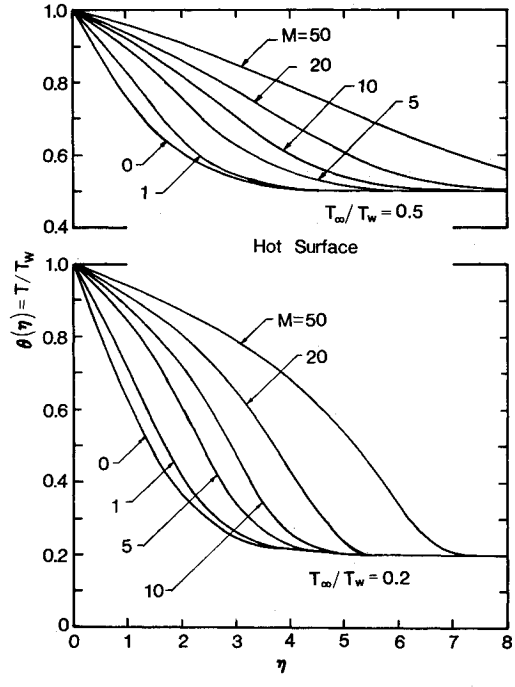

Fig. 6 Temperature profiles for a hot surface ($T_\infty/T_w = 0.2$ and 0.5).

It must be pointed out here that in deriving Eqs. (20) and (21) or Eqs. (27) and (28), the Rosseland approximation is assumed to be valid throughout the thermal boundary-layer thickness, including at the surface. In the work of Viskanta and Grosh,[11] the coefficient in the surface radiative heat flux term was changed from 4/3 to 2/3 for the region close to the wall in order to compensate for the Rosseland approximation. This approach could be applied easily to the present analysis, but it was not done in the numerical computations.

The local wall shear stress in the form of $\tau_w(x^2/5\mu\nu)(Gr_x^*/5)^{-3/5}$ as given by Eq. (26) is presented in Fig. 5. The solid lines are for the case of hot surface facing upward and the dotted lines are for the case of cold surface facing downward. In the abscissa, the temperature ratio T_∞/T_w is for the hot surface and T_w/T_∞ is for the cold surface. Both Gr_x^* and M are based on the appropriate reference temperature for each case. As can be seen from the figure, the wall shear stress increases with increasing thermal radiation interaction and decreases with increasing temperature ratio T_∞/T_w or T_w/T_∞. When $T_\infty/T_w = 1$, the wall shear stress becomes zero, as is to be expected, because no convection current exists under this condition. A comparison between the solid and dotted lines for a given value of M indicates that a hot surface results in a higher wall shear stress than a cold surface. This trend is consistent with the surface heat flux results shown in Figs. 3 and 4, and is also in conformity with the analogy between momentum and heat transfer.

It is also of interest to show how the thermal radiation interaction affects the temperature and velocity profiles. Representative temperature profiles $\theta = T/T_w$ for the case of hot surface are shown in Fig. 6 for $T_\infty/T_w = 0.2$ and 0.5. The curve for $M = 0.1$ is so close to that for $M = 0$ that it is not shown in the figure. It is clear from the figure that as the radiation interaction intensifies (i.e., as the value of M increases) radiation absorption in the boundary layer increases, causing the wall temperature gradient (the conductive wall heat flux) to decrease, as was pointed out earlier in the discussion of Fig. 1, and the thermal boundary-layer thickness to increase. The corresponding temperature profiles $\theta = T/T_\infty$ for the case of cold surface are illustrated in Fig. 7 for T_w/T_∞ of 0.2 and 0.5. As was mentioned in connection with Fig. 2, the effect of increasing radiation interaction for the cold surface is to decrease the conductive wall heat flux below the nonradiating medium case ($M = 0$) when $T_w/T_\infty > 0.5$ and to increase it above the nonradiating medium case when $T_w/T_\infty < 0.5$. This fact is observed again in Fig. 7. Also, since the thermal boundary-layer thickness always increases as the radiation interaction increases, the case of $T_w/T_\infty = 0.2$ demonstrates how the temperature profiles near the wall must cross each other for different values of M whenever $T_w/T_\infty < 0.5$. A comparison between Figs. 6 and 7 reveals that for the same value of M the thermal boundary-layer thickness is larger for the cold surface than for the hot surface.

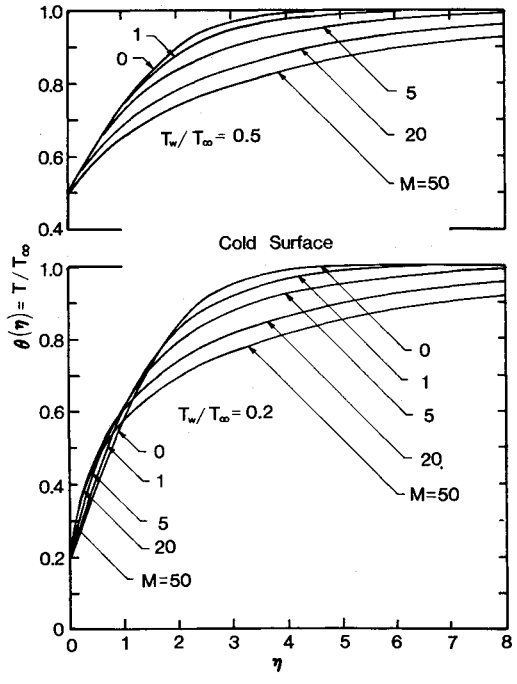

Fig. 7 Temperature profiles for a cold surface ($T_w/T_\infty = 0.2$ and 0.5).

The shape of the temperature profiles for various values of M for the case of hot surface facing upward, Fig. 6, indicates that the temperature gradient has a maximum value away from the surface. This is illustrated in the lower half of Fig. 8 for $T_\infty/T_w = 0.2$. The reason for this is the increased absorption of radiation in the region adjacent to the wall where the temperatures are high, which causes the temperature gradient near the wall to decrease. As the value of M increases, radiation interaction affects a larger region and the location of maximum temperature gradient shifts further away from the surface. Thus, for the case of hot surface facing upward, the local conductive heat flux is maximum at a position away from the wall, even though the local radiative heat flux is maximum at the wall [see the contribution of radiative heat flux in Eq. (27) as applied to a hot surface]. For the cold surface facing downward, on the other hand, the temperature gradient in the wall region is essentially constant for small values of M, but it decreases very rapidly for large values of M. This is the region in which the heat transfer is primarily by conduction, since the temperature level therein is much lower than T_∞. Thus, for the cold surface facing downward, maximum conductive heat flux occurs at the surface, but the maximum local radiative heat flux, which is a function of both the temperature and its gradient, exits somewhere away from the wall.

The velocity distribution as given by Eq. (22) contains Grashof number Gr_x that depends on $|T_w - T_\infty|$. To present the velocity profiles as functions of the radiation-conduction parameter M and the temperature ratio T_∞/T_w or T_w/T_∞, the Grashof number needs to be redefined based on a reference temperature T_0. With the use of modified Grashof number Gr_x^* as defined by Eq. (25), the expression for the velocity distribution becomes

$$\frac{ux}{5\nu}\left(Gr_x^*/5\right)^{-2/5} = \left|\frac{T_w - T_\infty}{T_0}\right|^{2/5}\frac{dF}{d\eta} \qquad (29)$$

where $T_0 = T_w$ for the hot surface and $T_0 = T_\infty$ for the cold surface. Representative velocity profiles in the form of $(ux/5\nu)(Gr_x^*/5)^{-2/5}$ for the case of hot surface with $T_\infty/T_w = 0.2$ are shown in Fig. 9. The curve for $M = 0.1$ is essentially

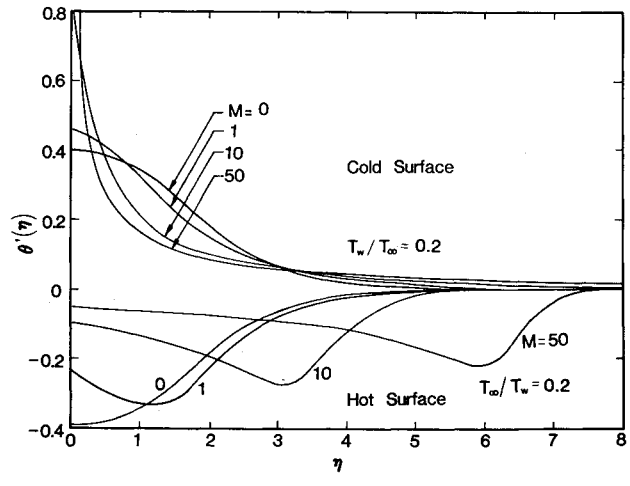

Fig. 8 Temperature gradient across the boundary layer (hot surface: $T_\infty/T_w = 0.2$; cold surface: $T_w/T_\infty = 0.2$).

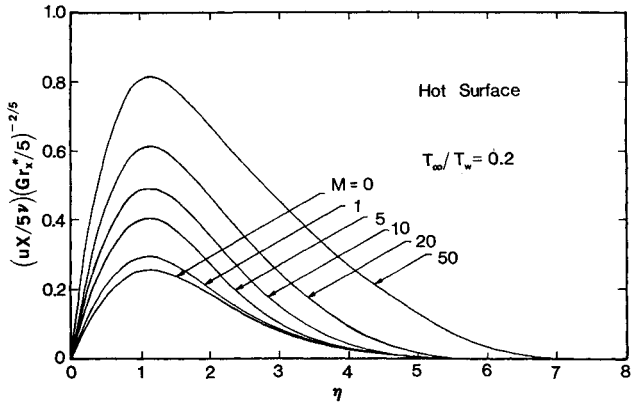

Fig. 9 Velocity profiles for a hot surface ($T_\infty / T_w = 0.2$).

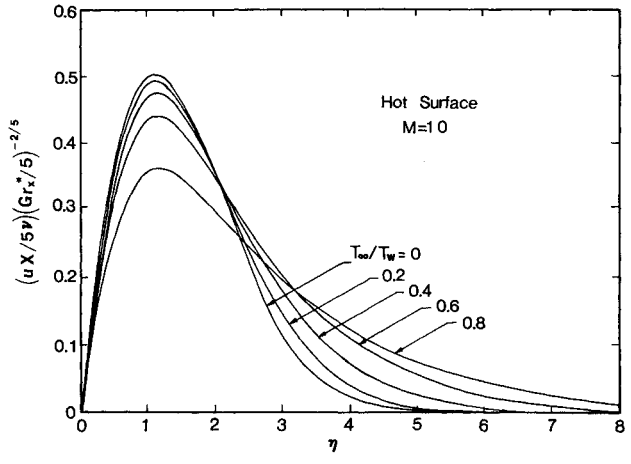

Fig. 10 Velocity profiles for a hot surface ($M = 10$).

coincident with the curve for $M = 0$ (i.e., for pure natural convection). As the interaction of thermal radiation intensifies (i.e., as the value of M increases), the velocity increases, with an accompanying increase in the velocity gradient at the wall and an increase in the flow boundary-layer thickness. Thus, thermal radiation enhances convective flow. To demonstrate the effect of temperature ratio T_∞/T_w on the velocity distribution, Fig. 10 has been prepared for $M = 10$. As is to be expected, the velocity decreases as the T_∞/T_w ratio increases from 0, attaining a zero velocity when T_∞/T_w approaches one. A decrease in the velocity is accompanied by a decrease in the velocity gradient at the wall, but an increase in the flow boundary-layer thickness. The velocity profiles for the case of cold surface are similar to those for the hot surface, with the exception that for the same value of M, the maximum velocity is smaller and occurs further away from the wall. In addition, the velocity decreases at a much slower rate toward the undisturbed ambient fluid, causing an increase in the boundary-layer thickness. In fact, the flow boundary-layer thickness is about three times larger for the cold surface when $M \geq 10$. To conserve space, the velocity profiles for the cold surface are not presented.

As a final note, it appears that there are no experimental data available for comparisons with the present predicted results.

Conclusion

In this paper the interaction of natural convection with thermal radiation has been studied for boundary-layer flow of an absorbing and emitting fluid over an isothermal semi-infinite flat plate. In the analysis, the radiative heat flux is represented by the Rosseland approximation. It has been found that thermal radiation plays a significant role in the net heat-transfer process. For both a hot surface facing upward and a cold surface facing downward, the thermal radiation interaction enhances the wall shear stress as well as the surface heat-transfer rate. The numerical results presented, though based on an approximate radiative flux analysis, are expected to provide the significant qualitative and quantitative behavior of the physical problem treated in the paper. They will serve as a basis for comparison with future studies in which a more exact representation needs to be made of the radiative heat flux.

Acknowledgment

The present study was supported in part by a grant from the National Science Foundation (NSF CME 79-19459).

References

[1] Ostrach, S., "An Analysis of Laminar Free-Convection Flow and Heat Transfer About a Flat Plate Parallel to the Direction of the Generating Body Force," NACA TN 2635, 1952.

[2] Pera, L. and Gebhart, B., "Natural Convection Boundary Layer Flow over Horizontal and Slightly Inclined Surfaces," *International Journal of Heat and Mass Transfer*, Vol. 16, 1973, pp. 1131-1146.

[3] Hasan, M.M. and Eichhorn, R., "Local Nonsimilarity Solution of Free Convection Flow and Heat Transfer from an Inclined Isothermal Plate," *Journal of Heat Transfer, Transactions of ASME*, Series C, Vol. 101, 1979, pp. 642-647.

[4] Chen, T.S. and Tzuoo, K.L., "Vortex Instability of Free Convection Flow over Horizontal and Inclined Surfaces," *Journal of Heat Transfer, Transactions of ASME*, Series C, Vol. 104, 1982, pp. 637-643.

[5] Cess, R.D., "The Interaction of Thermal Radiation with Free Convection Heat Transfer," *International Journal of Heat and Mass Transfer*, Vol. 9, 1966, pp. 1269-1277.

[6] Arpaci, V.S., "Effect of Thermal Radiation on the Laminar Free Convection from a Heated Vertical Plate," *International Journal of Heat and Mass Transfer*, Vol. 11, 1968, pp. 871-881.

[7] Cheng, E.H. and Ozisik, M.N., "Radiation with Free Convection in an Absorbing, Emitting and Scattering Medium," *International Journal of Heat and Mass Transfer*, Vol. 15, 1972, pp. 1243-1252.

[8] Hasegawa, S., Echigo, R., and Fukuda, K., "Analytical and Experimental Studies on Simultaneous Radiative and Free Convective Heat Transfer Along a Vertical Plate," *Proceedings of the Japanese Society of Mechanical Engineers*, Vol. 38, 1972, pp. 2873-2883 and Vol. 39, 1973, pp. 250-257.

[9] Bankston, J.D., Lloyd, J.R., and Novotny, J.L., "Radiation-Convection Interaction in an Absorbing-Emitting Liquid in Natural Convection Boundary Layer Flow," *Journal of Heat Transfer*, Transactions of ASME, Series C, Vol. 99, 1977, pp. 125-127.

[10] Sparrow, E.M. and Cess, R.D., "*Radiation Heat Transfer-Augmented Edition*," Hemisphere Publishing Corp., Washington, D.C., 1978, Chaps. 7 and 10.

[11] Viskanta, R. and Grosh, R.J., "Boundary Layer in Thermal Radiation Absorbing and Emitting Media," *International Journal of Heat and Mass Transfer*, Vol. 5, 1962, pp. 795-806.

[12] Cess, R.D., "The Interaction of Thermal Radiation in Boundary Layer Heat Transfer," *Proceedings of the Third International Heat Transfer Conference*, Vol. 5, 1966, pp. 154-163.